CHEMISTRY OF MATERIALS

pubs.acs.org/cm

Article

Supported Metal Nanohydrides for Hydrogen Storage

Estefania German,* Johanna Sandoval, Adrián Recio, Abdolvahab Seif, Julio A. Alonso, and María J. López

Cite This: *Chem. Mater.* 2023, 35, 1134−1147

Read Online

ACCESS | Metrics & More | Article Recommendations | Supporting Information

ABSTRACT: Adsorption of hydrogen on graphdiyne (GDY) and boron-graphdiyne (BGDY) doped with palladium clusters has been investigated by performing density functional calculations. Pd_6 fits well on the large holes of those porous layers, preserving its octahedral structure in GDY and changing it to a capped trigonal bipyramid structure in BGDY. Pd_6GDY adsorbs up to five H_2 molecules with sizable adsorption energies, two dissociated and three nondissociated. The dissociation barrier of H_2 on the Pd_6GDY cluster is 0.58 eV. Pd_6BGDY can adsorb up to six molecules, three dissociated and three nondissociated, and the dissociation barrier of H_2 on Pd_6BGDY is 0.23 eV. In both cases, the dissociation barriers are substantially smaller than the corresponding dissociation barriers on undoped GDY and BGDY. The Pd clusters saturated with hydrogen can be viewed as nanohydrides. Spilling of the adsorbed hydrogen atoms toward the GDY and BGDY substrates is hindered by large activation barriers. We then propose using BGDY and GDY layers as support platforms for metal nanohydrides. The amount of stored hydrogen using Pd as the dopant is below the target of 6% of hydrogen in weight, but replacing Pd by a lighter metal with similar or higher affinity for hydrogen would substantially enhance the storage.

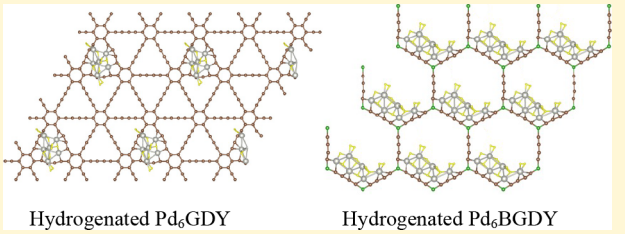

Downloaded via 168.196.25.125 on December 19, 2025 at 22:17:51 (UTC).
See https://pubs.acs.org/sharingguidelines for options on how to legitimately share published articles.

1. INTRODUCTION

In recent decades, substantial efforts have been made to facilitate the transition toward cleaner energy production systems in which CO_2 emissions to the atmosphere could be reduced. With this purpose in mind, hydrogen has become a subject of much interest because the amount of energy produced per unit mass during its combustion is higher than that of methane, gasoline, and coal,[1] plus the additional advantage of the absence of CO_2 emissions. As an energy carrier, hydrogen is especially attractive for using in vehicles, but its transport and storage is not free from risks due to its flammable nature.[2] This has led to many studies in search for safe and efficient conditions for its application. In this context, the study of materials with high hydrogen storage capacity has become an important research topic.[3] Targets have been established for materials to be used as hydrogen containers in vehicles: a storage capacity of 6% of hydrogen in weight, 40 g of hydrogen per liter of container should be achieved as short-term targets, 7.5% in weight, and 70 g per liter as long-term targets. Carbon materials in multiple forms, like porous carbons, activated carbon flakes, graphene, fullerenes, and carbon nanotubes, are outlined as candidates for storage.[3] Doping these materials with metal atoms, clusters, and nanoparticles significantly improves their hydrogen storage capacity.[4−12] One proposal to explain this improvement has been to assume a mechanism of spillover, in which the hydrogen molecules first adsorb on the surface of the metallic nanoparticle and dissociate, and then, the hydrogen atoms migrate toward the carbon substrate.[13] However, this mechanism has been analyzed in detail for the case of Pd nanoparticles supported on graphene by performing accurate atomistic dynamical simulations, and its validity has been questioned, because of the existence of large spillover barriers.[14,15] Sizable barriers have also been predicted from calculations for other supported transition metal clusters.[16−19] Palladium is, in fact, a promising metal for applications related to hydrogen storage because it can absorb large amounts of hydrogen in the form of palladium hydrides.[20] For this reason, the adsorption of hydrogen on free Pd nanoclusters[21−25] and on various types of carbon materials functionalized with palladium has been investigated.[6,7,26−34]

An interesting recently synthesized carbon material is graphdiyne (GDY), which is a layered structure formed by benzoic rings connected by diacetylenic carbon chains (see Figure 1). Its structure presents an ordered arrangement of large triangular holes.[35,36] Seif et al.[37] investigated the adsorption of palladium atoms and clusters on a GDY layer, concluding that GDY can be used as an efficient substrate and reporting the triangular hollow regions of the GDY as preferential sites for the adsorption of Pd clusters. A new material related to GDY is boron-graphdiyne (BGDY). In this

Received: October 11, 2022
Revised: January 17, 2023
Published: January 27, 2023

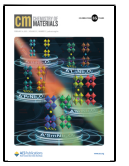

© 2023 The Authors. Published by American Chemical Society

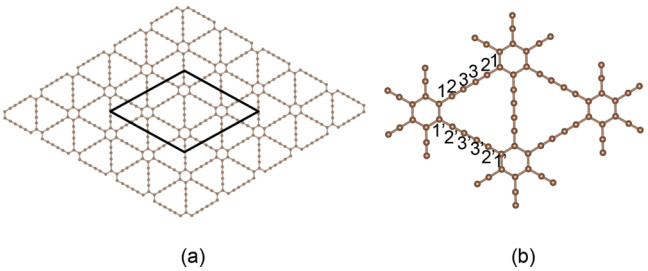

Figure 1. (a) Optimized structure of graphdiyne (GDY). (b) Enlarged view of the unit cell used in the calculations; carbon atoms along chains joining the benzoic rings are labeled.

two-dimensional (2D) structure, boron atoms replace the hexagonal carbon rings in the GDY layer. Boron has three valence electrons and binds with three diacetylenic chains, forming a 2D honeycomb lattice with big hexagonal holes, as shown in Figure 2. BGDY was experimentally synthesized by a

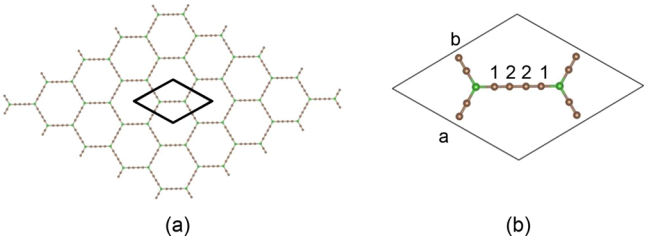

Figure 2. Left panel: honeycomb structure of BGDY. Right panel: unit cell and labeling of carbon atoms. Boron and carbon atoms are represented by green and brown spheres, respectively.

bottom-up strategy.[38] The adsorption of transition metal atoms and clusters on BGDY layers has been recently studied.[39] The adsorption of hydrogen on GDY and BGDY decorated with light sp and 3d atoms (Li, Na, K, Ca, Sc, and Ti on GDY; Li, Na, K, and Ca on BGDY) has been computationally investigated by Hussein and coworkers,[40,41] and the results are encouraging. The effect of substitutional N and S doping on the hydrogen storage capacity of GDY has also been analyzed.[42] A number of studies have reported computational investigations of hydrogen storage on materials closely related to GDY: specifically, graphyne, a layered material (although not yet synthesized) with a structure similar to that of GDY in Figure 1 but with shorter carbon chains and materials related to graphyne.[43−47] The effect of decoration (with alkali and alkaline-earth atoms) and substitutional doping (with Al, N, and B) on hydrogen adsorption by those materials was studied in detail in those studies. Understanding the details of the interaction between hydrogen and supported active metal atoms and nanoparticles is also relevant to develop good electrocatalysts for the hydrogen evolution reaction.[48,49]

The objective of this work is to investigate the adsorption of hydrogen on palladium clusters, specifically Pd_6, supported on GDY and BGDY layers, to explore the possibilities of these doped carbon materials in hydrogen storage. One of the advantages of GDY and BGDY over other carbon materials for the purposes of gas storage is the lower weight. One reason for choosing palladium is that experiments by Contescu and coworkers[6,7,50−53] and others[30,32] reported an enhancement of hydrogen storage when doping carbon materials with Pd. A second reason is that we have previously performed calculations to study the effect of this dopant on different carbon materials[26−29,37,39] and have analyzed the hydrogen spillover process.[14,15] For this purpose, we perform accurate calculations using the formalism of density functional theory (DFT).[54] DFT is nowadays being used as a tool for the search and discovery of materials with new or targeted properties.[55,56] We find that the Pd clusters on the light GDY and BGDY substrates can be used to build two-dimensional platforms of metal nanohydrides of potential interest as hydrogen storage materials. The results also suggest using metals lighter than palladium to enhance storage.

2. COMPUTATIONAL METHODOLOGY

The theoretical calculations have used the Kohn-Sham DFT[54] as implemented in the Quantum Espresso computational package.[57,58] Electronic exchange and correlation effects were approximated by the Perdew-Burke-Ernzerhof (PBE) generalized gradient (GGA) functional.[59] Projector-Augmented Wave (PAW) pseudopotentials[60,61] were used to describe the interaction between valence and core electrons, and three valence electrons were taken for boron, four for carbon, ten for palladium, and one for hydrogen. Dispersion effects were included using Grimme's DFT-D3 method.[62,63] A cut-off energy of 45 Ry was employed for the basis of plane waves used to expand the electronic wave functions. The corresponding cut-off for the electron density was 360 Ry in GDY and 350 Ry in BGDY. The unit cells for GDY and BGDY are shown in Figures 1 and 2, respectively; those cells are large enough to avoid the interaction between the adsorbed Pd clusters. The Brillouin zone in the reciprocal space was sampled in both materials with a 3 × 3 × 1 Monkhorst−Pack grid,[64] which allows for well converged total energies. In the structural relaxation calculations to find the lowest energy configurations in the clean and adsorbed systems, a value of 0.0002 Ry was selected as the criterion for energy convergence, and it was also required that the forces acting on each of the atoms are below 0.0019 Ry/Å. All calculations were carried out in spin-polarized mode.

Previous to the study of the adsorption of hydrogen, the structures of the GDY and BGDY substrates were optimized. Then, a Pd_6 cluster was deposited on the substrate layers, and hydrogen was adsorbed next. The adsorption energy of the palladium cluster on GDY is calculated from the equation:

$$E_{ads}\,(Pd_6) = E_{GDY} + E_{Pd6} - E_{Pd6GDY} \quad (1)$$

where E_{GDY}, E_{Pd6}, and E_{Pd6GDY} are the total energies of clean GDY, the free Pd_6 in its ground state structure, and the system formed by the Pd_6 adsorbed on GDY, respectively. A similar equation applies to the adsorption energies of Pd_6 on BGDY. To determine the adsorption energy of an H_2 molecule on Pd_6GDY, the following equation is used:

$$E_{ads}\,(\text{first } H_2) = E_{Pd6GDY} + E_{H2} - E_{H2/Pd6GDY} \quad (2)$$

where $E_{H2/Pd6GDY}$ is the total energy of the system formed by H_2 adsorbed on Pd_6GDY, and E_{H2} is the energy corresponding to the isolated H_2 molecule, determined using the same parameters and the same cell as for the other systems. If the adsorbed molecule is dissociated (2H), the corresponding adsorption energy is given by

$$E_{ads}\,(\text{first } 2H) = E_{Pd6GDY} + E_{H2} - E_{2H/Pd6GDY} \quad (3)$$

https://doi.org/10.1021/acs.chemmater.2c03106
Chem. Mater. 2023, 35, 1134−1147

where the reference is again formed by Pd_6GDY and the isolated H_2 molecule, and this allows a comparison of molecular and dissociative adsorption. Similar equations apply to BGDY.

3. GDY AND BGDY LAYERS

A supercell consisting of a periodic repetitive structure of the GDY unit cell formed by 72 carbon atoms can be seen in Figure 1a. The cell parameter in the z direction (perpendicular to the layer) was fixed at 14 Å, large enough to avoid the interaction between periodic images. To identify the different carbon atoms of the structure, these have been assigned an integer number according to their position (Figure 1b), assigning the same number to equivalent carbon atoms within the same linear chain. To distinguish between equivalent atoms in different chains, the atoms in the second chain are marked with a prime superscript. The optimized distance between the centers of neighbor hexagonal benzoic cycles is 9.449 Å. The lattice constant, which is twice this value, agrees with other results previously reported.[35,37,65] The lengths of the bonds along the linear chains $C^1{-}C^2{\equiv}C^3{-}C^3{\equiv}C^2{-}C^1$ vary according to the type of bond, being 1.231 Å for the triple bonds $C^2{\equiv}C^3$, and 1.338 Å for the single bond $C^3{-}C^3$. The bond distance between the carbon atom of the hexagonal ring and the first acetylene carbon ($C^1{-}C^2$) is 1.395 Å. Regarding the separation between equivalent atoms on neighbor linear chains of the triangular holes, the distances for atoms near the hexagons are $d(C^2{-}C^{2\prime})$ = 2.824 Å and $d(C^3{-}C^{3\prime})$ = 4.056 Å.

BGDY is a layered framework related to graphdiyne (GDY). It is formed by a network of boron atoms connected by carbon chains containing diacetylenic $-C{\equiv}C{-}C{\equiv}C-$ linkages (see Figure 2). The layer structure displays an ordered arrangement of hexagonal holes, with the two ends of the carbon chains (which form the hexagon sides) linked to the boron atoms. The BGDY layer was modeled using a repetitive cell containing 14 atoms (12 C atoms and 2 B atoms) and a vacuum spacing of 20 Å in the direction perpendicular to the layer. The optimized lattice constant ($a = b$ in Figure 2) is 11.847 Å.

4. PD_6 DEPOSITED ON GDY AND BGDY

Free Pd_6 is an octahedron.[12] In order to simulate the results of a soft-landing experiment,[66] Pd_6 was placed on GDY at different locations and with different orientations of the cluster on the substrate, and all those configurations were optimized to find the structure with the lowest energy. This procedure is likely to deliver the structures achievable in soft-landing cluster deposition experiments at low or moderate temperatures. The calculations led to the lowest energy configuration (ground state) shown in panel (a) of Figure 3. This Figure shows in panel (b) a low-lying structure close in energy to the ground state. That structure will be useful in the discussion on hydrogen adsorption. In the relevant cases, like those in Figure 3a,b, the supported cluster sits inside the triangular hole and fits rather well there, although some distortion of the three carbon chains forming the hole can be appreciated. To identify each Pd atom, these have been labeled Pd1, Pd2, ... Pd6 in the panels of Figure 3. The Pd cluster essentially maintains the octahedral structure, and configurations (a) and (b) only differ in the orientation of the octahedral cluster with respect to the GDY layer.

We begin by describing the structure of panel (b). The Pd_6 cluster rests on a triangular face in contact with the GDY layer,

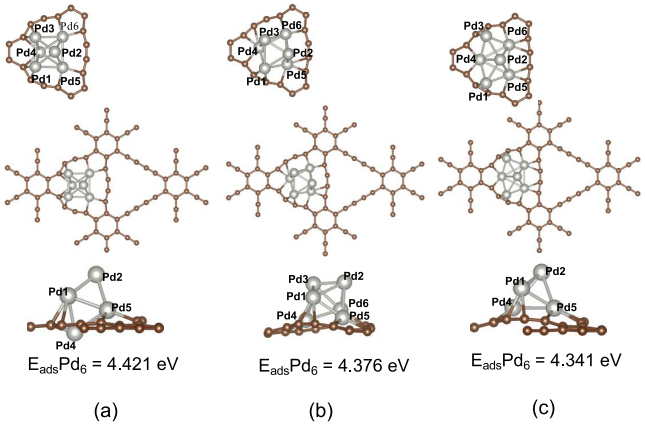

Figure 3. Top and lateral views of the lowest energy structure (a) and two low-lying isomeric structures, (b, c), of Pd_6 adsorbed on GDY. Adsorption energies are indicated. C and Pd atoms are represented by brown and gray spheres, respectively. Different Pd atoms are labeled Pd1, Pd2, ... Pd6.

the face formed by the atoms labeled Pd4, Pd5, and Pd6. This triangular face is oriented in the same way as the triangular hole, but the face is slightly tilted with respect to the GDY plane. The vertical distances of these three atoms over the GDY layer are 0.51, 0.62, and 1.13 Å, respectively. The octahedral structure of Pd_6 is, however, a bit distorted, and the bond between atoms Pd4 and Pd5 is broken. The adsorption energy of the cluster in this configuration is E_{ads} (Pd_6) = 4.376 eV, which results mainly from the bonds between atoms Pd4, Pd5, and Pd6 and carbon atoms (the Pd−C bond distances are between 2.02 and 2.20 Å). However, because of the tilted orientation of the cluster, also atom Pd1 builds bonds with C atoms (bond distances of 2.23 and 2.27 Å). The adsorption energy is substantially larger than the adsorption energy of Pd_6 on graphene and not far from the binding energy of Pd_6 to a graphene vacancy.[12] The dispersion contribution to the adsorption energy is 0.67 eV, which amounts to 15%.

In panel (a), which shows the lowest energy structure of Pd_6GDY, the Pd_6 cluster maintains the octahedral structure with quite small distortions. The tilt of the triangular face is larger than that shown in panel (b), the orientation of the cluster is such that one axis of the octahedron is nearly perpendicular to the GDY plane (angle = 83°), and atom Pd4 is slightly below the GDY plane (z = − 0.28 Å). The adsorption energy is E_{ads} (Pd_6) = 4.421 eV; that is, this configuration is 0.045 eV more stable than that of panel (b). The reason is that the orientation of Pd_6 in panel (a) allows forming additional bonds between Pd and C atoms, and this bonding is able to compensate for the larger deformation appreciable in the carbon chains. It appears that a simple reorientation of the Pd_6 cluster with respect to the GDY layer leads from structure 3(b) to 3(a). These two structures represent, however, different local minima in the potential energy surface of the system, and Figure S1 of the Supplementary Information shows the minimum energy path for the structural transformation from structure 3(b) to 3(a), calculated by the nudged elastic band (NEB) method.[67] The activation barrier for the reorientation of the adsorbed Pd_6 cluster is small, 0.18 eV. Since structures 3(a) and 3(b) are so close in energy, differing only in the orientation of the metal cluster with respect to the GDY layer, and have low interconversion energy barriers, one can expect that both

https://doi.org/10.1021/acs.chemmater.2c03106
Chem. Mater. 2023, 35, 1134−1147

structures will be present in soft-landing deposition of Pd_6 clusters.

The bonds formed between cluster atoms and substrates may prevent arriving at other, distorted structures, in the soft-landing cluster deposition experiments. Previous experience indicated that the adsorption of small molecules on the surface of free and supported metal clusters may induce structural transformations in the cluster.[68−70] Since investigating the adsorption of hydrogen on supported Pd_6 is the main objective of this work, we obtained feedback from that study. That is, cluster structures found in the process of adsorbing hydrogen (see Section 6) were taken (with hydrogen suppressed) as initial structures for a more extensive structural optimization of Pd_6GDY. As a result, other configurations were found, and one of these is shown in panel (c) of Figure 3. The cluster Pd_6 also sits inside the triangular hole. The structure of Pd_6 in panel (c) is different from those of panels (a, b) and can be viewed as an incomplete pentagonal bipyramid. It can be obtained by starting from the structure in panel (a) and breaking the bond between atoms Pd1 and Pd3. The adsorption energy is 4.341 eV, close to those of panels (a, b). However, Pd_6GDY structures more stable than those of Figure 3a,b were not discovered. The conclusion from Figure 3 is that different isomeric forms with similar stability can be present after the deposition of Pd_6 on GDY and could form in atom-by-atom deposition experiments. This is expected to be also the case for other small clusters.

The hexagonal holes in BGDY are larger than the triangular holes of GDY. The most stable structure of Pd_6 adsorbed on BGDY is shown in Figure 4. The original octahedral structure

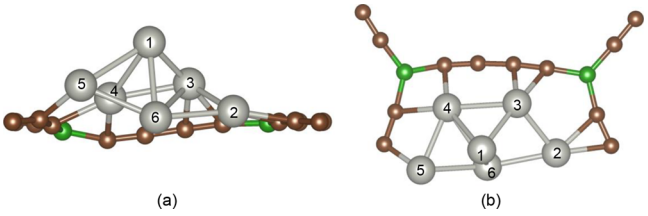

Figure 4. Lateral and top views of the lowest energy configuration of Pd_6 adsorbed on the BGDY layer. C, B, and Pd atoms are represented by brown, green, and gray spheres, respectively. Pd atoms are labeled.

of free Pd_6 changes to form a capped trigonal bipyramid with the capping Pd atom, labeled as Pd2 in the Figure, bonded in a bridge position to the two atoms, Pd3 and Pd6, of an edge of the bipyramid. The cluster is situated between two adjacent corners of the hexagonal hole, and four Pd atoms form bonds with C atoms. The position of the cluster is displaced a bit toward one corner, the left corner in the view of Figure 4. The adsorption energy of Pd_6 is 4.21 eV, slightly smaller than the adsorption energy on GDY.

5. HYDROGEN ADSORPTION ON CLEAN GDY AND BGDY

As a preliminary study, we consider the adsorption of hydrogen on the clean substrates, GDY and BGDY. The results can be compared with work on the adsorption of hydrogen on clean graphene and can also serve as a reference for comparison with adsorption on GDY and BGDY doped with palladium. Molecular adsorption of H_2 on BGDY occurs preferentially above the B−C≡C−C≡C−B chains. The adsorption energies,

$$E_{ads}(H_2) = E_{BGDY} + E_{H2} - E_{H2/BGDY}, \quad (4)$$

where $E_{H2/BGDY}$ is the energy of the system formed by H_2 adsorbed on BGDY, are small, close to 0.05 eV, and the distances between the H_2 molecules and the C chains are slightly above 3 Å. These values are similar to the adsorption energies and distances of H_2 adsorbed on graphene.[71,72] Dissociative adsorption is energetically possible. The dissociative adsorption energies are 1.63 eV/molecule, and the H atoms are attached to neighbor C atoms. However, the dissociation barrier is quite large (1.96 eV), and direct H_2 dissociation on clean BGDY is unlikely. The barrier calculated by the NEB method is shown in Figure S2.

$$E_{ads}(2H) = E_{BGDY} + E_{H2} - E_{2H/BGDY}. \quad (5)$$

The adsorption energies of H_2 on GDY are small as well, 0.07 eV, and the hydrogen molecules are located approximately over the center of the triangular holes of the GDY layer, at distances from the C atoms slightly above 3 Å. Hydrogen molecules can also be adsorbed over the center of the benzoic hexagons (adsorption energies of 0.06 eV) and on top of C1−C2 bonds (adsorption energies of 0.05 eV). Dissociative adsorption is possible and the most favorable configuration shows the two H atoms attached to neighbor carbon atoms of the chains, with a large adsorption energy of 1.77 eV/molecule. However, the dissociation barrier is quite large (1.62 eV), and direct H_2 dissociation on clean GDY is not expected to happen. The barrier calculated by the NEB method is shown in Figure S3. The high H_2 dissociation barriers on GDY and BGDY contrasts with the low barriers on the edges of graphene nanoribbons.[73] This difference is due to the unsaturated dangling bonds on the nanoribbons, which make these highly reactive.

6. HYDROGEN ADSORPTION IN PD-DOPED GDY

We first consider a single Pd atom on GDY. The Pd atom prefers to rest in the hollow regions of the GDY plane near the corners of the triangular holes, forming bonds with atoms C2, C3, C2′, C3′ (see Figure 1) of two adjacent carbon chains.[37] Its binding energy is 2.60 eV. The adsorption energy of an H_2 molecule on this Pd atom is 0.39 eV, and dissociative adsorption of the molecule is not stable. It is useful to compare these results with those for a Pd atom on graphene.[26] The most favorable position of the Pd atom on graphene is in a bridging position above a C−C bond, with a binding energy of 1.09 eV, and H_2 is adsorbed on this Pd atom with an energy of 0.96 eV. Thus, Pd is attached more strongly to GDY (forming bonds with four C atoms), as compared to graphene (forming bonds with two C atoms). The bonding capacity of the Pd atom is nearly exhausted in GDY, and consequently, the adsorption energy of H_2 is weaker. In summary, the strength of the bonding between the Pd atoms and H_2 is sensitive to the chemical environment of the Pd atoms because that environment can consume part of the bonding capacity of the Pd atoms.

Previous work on hydrogen adsorption on Pd_n clusters supported on other carbon substrates (pristine and defective graphene) revealed that molecular adsorption occurs on top of the Pd atoms.[26,29,68] Based on this observation, we explored H_2 adsorption on the different Pd atoms of the structures of Pd_6GDY in panels (a, b) of Figure 3. The most stable adsorption occurs for the H_2 molecules on top of the Pd atoms positioned at high vertical distances from the GDY layer, and

https://doi.org/10.1021/acs.chemmater.2c03106
Chem. Mater. 2023, 35, 1134−1147

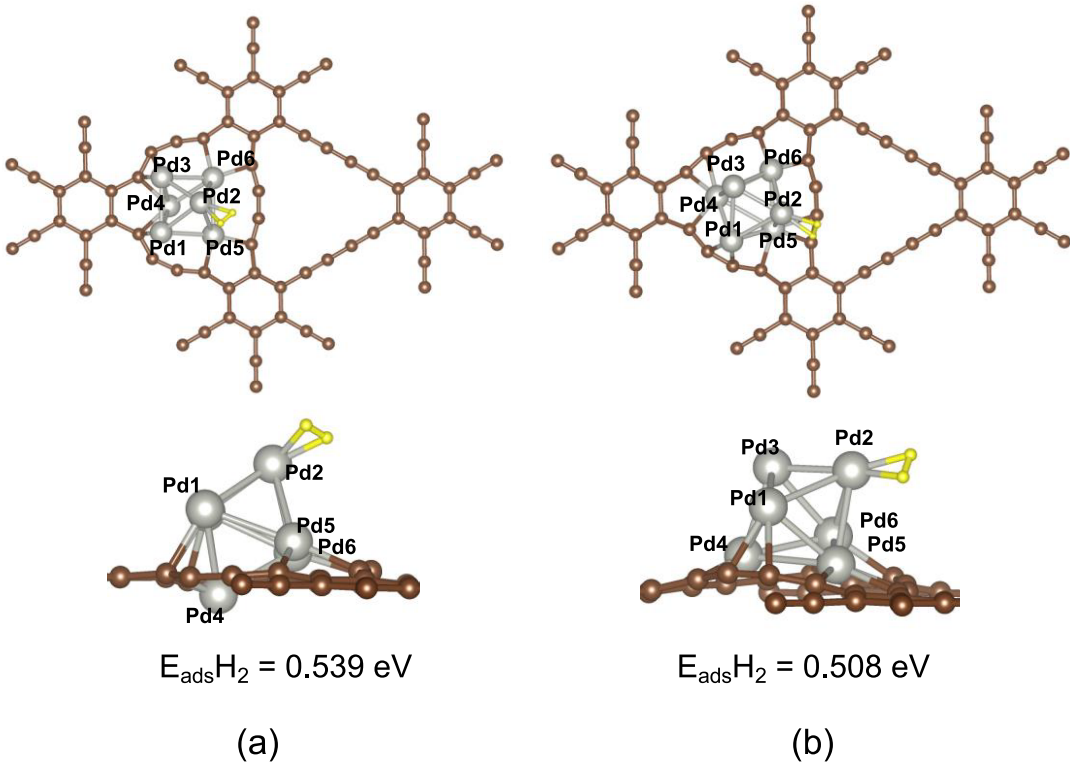

Figure 5. Top and lateral views of the lowest energy configurations for the molecular adsorption of H_2 on the two isomeric forms of Pd_6GDY, as shown in Figure 3a,b. C, Pd, and H atoms are represented by brown, gray, and yellow spheres, respectively.

Figure 5 shows the most stable configuration in each of those cases. The adsorption energies are 0.539 and 0.508 eV, respectively, values consistent with the adsorption energy of H_2 on Pd_6 anchored to a graphene vacancy, which is 0.77 eV.[74] The difference reflects the effect of different carbon substrates. It should be noticed that in calculating the molecular adsorption energy using eq 2, the term E_{Pd6GDY} represents the energy of clean Pd_6GDY in its lowest energy structure, as shown in Figure 3a. Consequently, the adsorption energies indicate that the lowest energy configuration after molecular adsorption of H_2 is the one shown in Figure 5a, which comes from the structure shown in Figure 3a. However, the total energy difference between the configurations of Figure 5a,b is only 0.031 eV, and both will be competitive in practice. In fact, the difference in total energy between the two systems with adsorbed hydrogen (0.031 eV) is lower than the difference in energy between the two clean systems (0.045 eV).

Recalling the labels introduced in Figure 3, the H_2 molecule is adsorbed on the Pd2 atom, as shown in Figure 5b, and the adsorption energy on the Pd3 atom is the same. These are Pd atoms which do not form bonds with C atoms. From previous work[29] on Pd clusters anchored to graphene vacancies, it is known that the adsorption of H_2 is less favorable on Pd atoms bonded to the C atoms of the substrate, as compared to adsorption on Pd atoms nonbonded to C atoms. The other four Pd atoms of the cluster form both Pd−Pd and Pd−C bonds, and as expected, the adsorption energies are smaller: 0.288 eV on Pd1, 0.059 eV on Pd6, and adsorption were not stable on Pd4 and Pd5. The differences between Pd2 and Pd3 on one side, and the rest of the Pd atoms on the other, arise from two sources. One is that reactivity decreases with increasing atomic coordination of the host atom,[70,75,76] and the other is a simple steric effect. Turning to Figure 5a, H_2 adsorption energies of 0.539 eV are obtained on the top of atom Pd2, which forms bonds with other Pd atoms only. In a second group, formed by atoms Pd1, Pd3, and Pd4, the adsorption energies are smaller (0.507 eV for Pd1 and Pd3, and 0.466 eV for Pd4), and adsorption is not stable on Pd5 and Pd6. Again, the difference between groups is explained by atomic coordination and steric effects. The bond lengths d(H−H) of H_2 molecules adsorbed on Pd_6GDY are close to 0.84 Å, a bit elongated with respect to the bond length of free H_2 (the calculated bond length is 0.75 Å, and the experimental one is 0.76 Å), so the H_2 molecules can be considered to be activated. H−Pd bond lengths vary between 1.76 and 1.78 Å, similar to those for H_2 adsorption on Pd_6Graphene.[29] Molecular adsorption of H_2 on the carbon chains is weaker, with binding energies below 0.1 eV and the molecule located at distances of 3 Å or more from the C atoms. This means that the presence of Pd_6 does not affect the adsorption of molecular hydrogen on the GDY framework.

To investigate the dissociative adsorption of the hydrogen molecule, we started with the Pd_6GDY configurations of Figure 3a,b, and based again on previous experience,[26,29,68] the H atoms were initially placed in bridge positions on top of the bonds between Pd atoms. The bonding between H and Pd atoms caused in some cases structural changes in Pd_6. The lowest energy structure of the dissociated molecule (H + H) is given in Figure 6b, which shows that the shape of the Pd_6 cluster has changed from the original octahedral structure to a slightly deformed incomplete pentagonal bipyramid. The two H atoms are located in bridge positions above the Pd1−Pd2 and Pd2−Pd3 bonds, with Pd−H distances in the range of 1.68−1.88 Å. The dissociative adsorption energy in the configuration of Figure 6b is E_{ads} (2H) = 1.330 eV, much larger than the molecular adsorption energies. Distorting the

https://doi.org/10.1021/acs.chemmater.2c03106
Chem. Mater. 2023, 35, 1134−1147

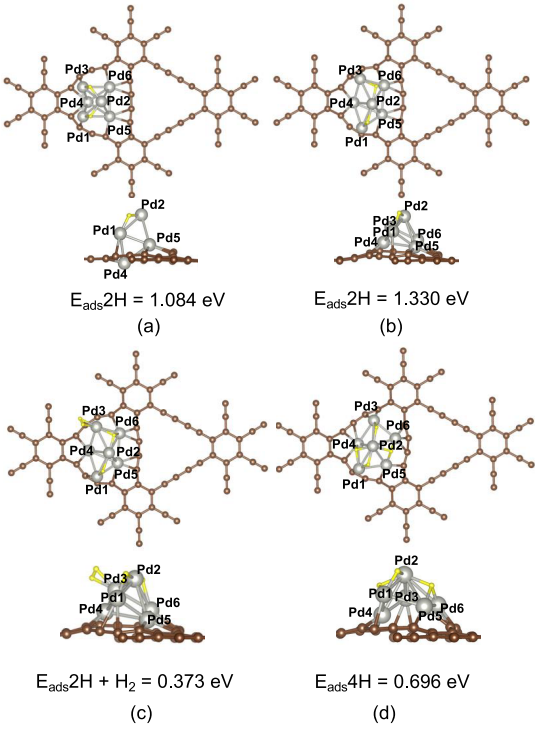

Figure 6. Panels (a) and (b) show two configurations of the dissociated (H + H) hydrogen molecule on Pd_6GDY. Those configurations are related to panels (a, c) of Figure 3. Panels (c, d) show molecular and dissociative adsorption configurations, respectively, for a second hydrogen molecule on Pd_6GDY with a pre-adsorbed dissociated molecule. Top and lateral views are shown in all cases. C, Pd, and H atoms are represented by brown, gray, and yellow spheres, respectively.

structure of Pd_6 in Figure 3a to arrive at that of Figure 3c has an energy cost of 0.08 eV. The dissociative adsorption energy of H_2 on the Pd_6GDY configuration of Figure 3a is 1.084 eV (this configuration is shown in Figure 6a), and the difference in adsorption energies, 1.330−1.084 = 0.246 eV, shows that the configuration of Figure 6b is more stable even after affording for the energy cost of the structural distortion.

The dissociation path connecting the initial configuration with H_2 adsorbed on Pd_6GDY given in Figure 5a and the final configuration, corresponding to the dissociated molecule given in Figure 6b, exhibits an activation barrier of 0.58 eV. This barrier is substantially smaller compared to the dissociation barrier of H_2 on clean GDY (1.62 eV; see Section 5). A few snapshots along the dissociation path are shown in Figure 7. The process of dissociation is interesting. H_2 first promotes the structural transformation of Pd_6 from the octahedron to the incomplete pentagonal bipyramid. H_2 is dissociated in the saddle point configuration but then returns to its original molecular state in image 4. In fact, the structure of Pd_6GDY in this image is essentially the same as the structure shown in Figure 3c. In a second step, dissociation of the H_2 molecule occurs, with a quite low barrier of 0.09 eV and no change in the cluster structure.

Starting with the dissociated configuration of Figure 6b, a second hydrogen molecule was added, and the two cases of dissociated (2H) and molecular (H_2) adsorption were studied. The adsorption energy of the second molecule in the dissociated case is defined.

$$E_{ads}\ (\text{second: 2H}) = E_{2H/Pd6GDY} + E_{H2} - E_{4H/Pd6GDY}, \tag{6}$$

where $E_{2H/Pd6GDY}$ and $E_{4H/Pd6GDY}$ represent the energies of the system with one and two dissociated molecules, respectively. In a similar way, the adsorption energy when the second adsorbed molecule is not dissociated can be written.

$$E_{ads}\ (\text{second: } H_2) = E_{2H/Pd6GDY} + E_{H2} - E_{H2(2H)/Pd6GDY}. \tag{7}$$

Similar definitions can be made for the adsorption of a third molecule, etc. The results for molecular and dissociated adsorption of the second molecule are given in Figure 6c,d, respectively. Molecular adsorption of the second H_2 molecule preserves the geometry that Pd_6 had in $2H/Pd_6GDY$. The molecule can be adsorbed on top of atoms Pd1, Pd2, and Pd3 and the most stable adsorption occurs on Pd3, with E_{ads} (H_2) = 0.373 eV, and bond lengths d(H−H) = 0.824 Å, and d(Pd−H) of 1.816 and 1.839 Å. H_2 is adsorbed on Pd1 and Pd2 with E_{ads} (H_2) = 0.259 and 0.323 eV, respectively. In contrast,

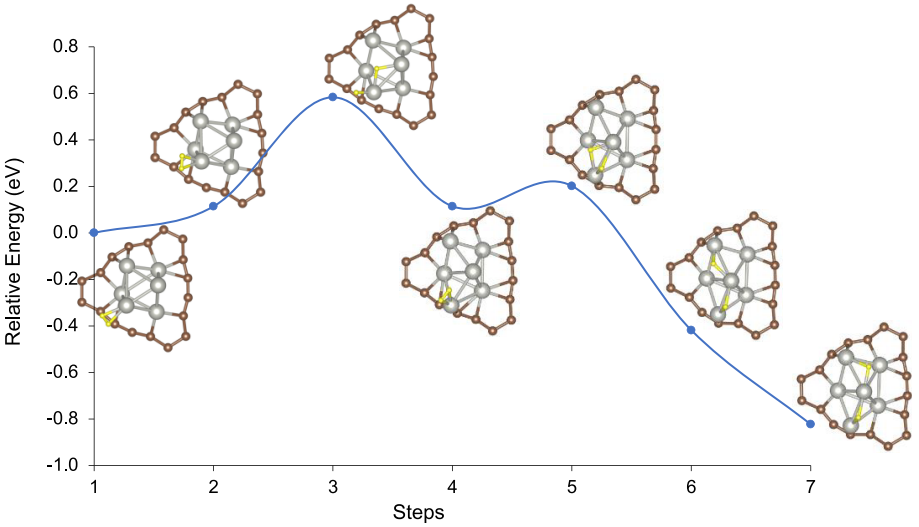

Figure 7. Energy curve and structural snapshots along the dissociation path of H_2 on Pd_6GDY. C, Pd, and H atoms are represented by brown, gray, and yellow spheres, respectively.

https://doi.org/10.1021/acs.chemmater.2c03106
Chem. Mater. 2023, 35, 1134−1147

dissociative adsorption of the second molecule induces additional changes in the structure of Pd_6. Displacements of some Pd atoms are observed, and five Pd atoms maintain bonds with C atoms. Two of those atoms, Pd4 and Pd5, are located at the corners of the triangular hole, and the other three, Pd1, Pd3, and Pd6, are placed near the middle of the acetylenic chains. One of the newly added H atoms is located in a bridge position above the Pd1−Pd2 bond and the other on a hollow site above the triangular Pd2−Pd5−Pd6 face. The adsorption energy of the second dissociated molecule is 0.696 eV, and dissociated adsorption is again favorable with respect to molecular adsorption.

Upon addition of these two dissociated hydrogen molecules, this system can adsorb three more nondissociated hydrogen molecules before reaching saturation. The adsorption energy of each successively added molecule, and the corresponding minimum energy structures are shown in Figure 8. The Pd_6 cluster does not suffer significant structural changes. Three hydrogen molecules are adsorbed on top of Pd atoms (Pd1, Pd2, and Pd3), and the H−Pd bond distances are between 1.85 and 1.92 Å. The successive adsorption energies and adsorption mode (molecular or dissociative) of the five H_2 molecules that Pd_6GDY can adsorb are listed in Table 1.

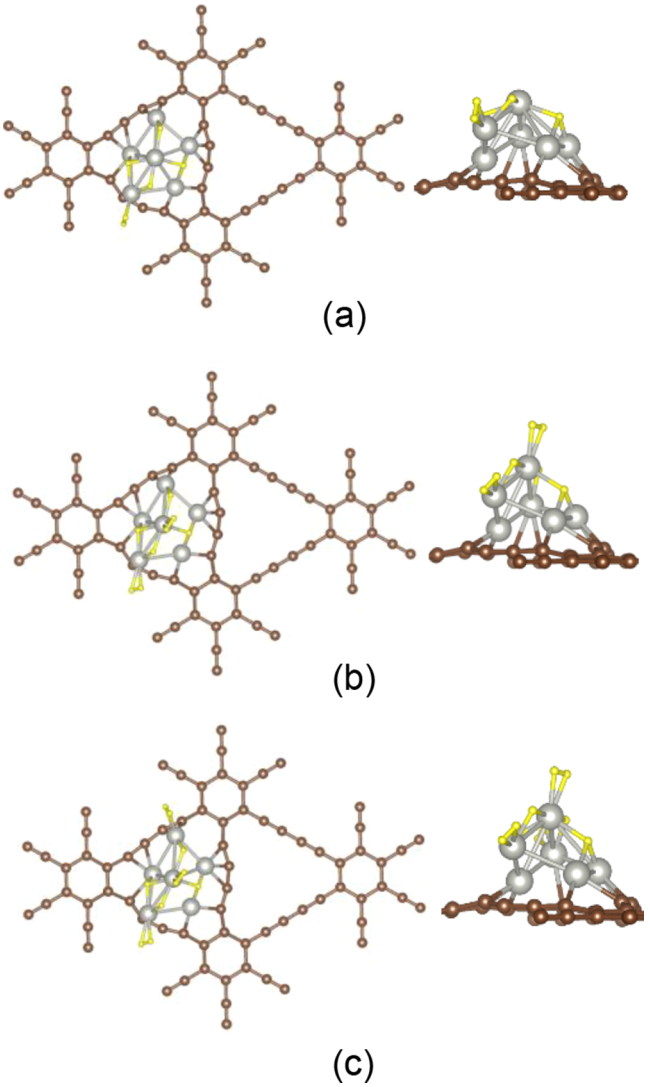

Figure 8. Minimum energy configurations of Pd_6GDY with an increasing number of H_2 molecules adsorbed: (a) two dissociated and one non-dissociated, (b) two dissociated and two non-dissociated, (c) two dissociated and three non-dissociated. C, Pd, and H atoms are represented by brown, gray, and yellow spheres, respectively.

Table 1. Adsorption of H_2 Molecules on Pd_6GDY: Number N of Adsorbed Molecules, Adsorption Mode (Molecular or Dissociative Adsorption), and Adsorption Energy of the Last Molecule, E_{ads} (Last)

N	adsorption mode (last molecule)	E_{ads} (last) (eV)
1	dissociated	1.330
2	dissociated	0.696
3	molecular	0.315
4	molecular	0.344
5	molecular	0.195

For comparison, Pd_6 anchored to a vacancy in graphene can adsorb nine molecules, three dissociated and six non-dissociated.[12,15,29] Our proposed explanation is that Pd_6 fits better in the space of the triangular holes of GDY, as compared to the smaller graphene vacancies. The more efficient fitting results in a larger number of Pd−C bonds in GDY, so a part of the bonding capacity of the Pd atoms is exhausted, and consequently, the affinity of the Pd_6 cluster for hydrogen is lower.

The changes in the electronic structure of GDY induced by the adsorption of Pd clusters were studied earlier,[37] and it was found that the main effect is lowering of the value of the electronic gap. Here, we have studied the additional effects due to the presence of hydrogen. Figure 9 shows a comparison of the densities of states (DOS) of Pd_6GDY, $2(H_2)/Pd_6$GDY, and $2(2H)/Pd_6$GDY, that is, Pd_6GDY clean, and hosting two nondissociated or two dissociated hydrogen molecules, respectively. The total DOS in each panel is separated in spin up and spin down components. The DOS projected on the Pd and H atoms are characterized by different colors. The electronic states corresponding to the nondissociated H_2 molecule (panel (b) of Figure 9) are well localized and clearly distinguished at a binding energy of 7.7 eV below the Fermi energy. The perturbation of the electronic structure of Pd_6GDY is otherwise quite small. In contrast, in the case of dissociated molecules (panel (c) of Figure 9), the H atoms form bonds with the Pd atoms of the metal cluster, and the electronic states are strongly hybridized in the energy region between −5 and −7 eV. The different types of bonding are also appreciated in the electron density. Figure S4 of the Supporting Information shows that the electric charges of the nondissociated H_2 molecule and the neighbor Pd atom become polarized. Instead, the H atoms of the dissociated hydrogen molecules sit in regions rich in electronic charge.

It is desirable to study the possibility of the spillover mechanism in Pd_6GDY saturated with hydrogen ($4H + 3H_2$). For this purpose, we have calculated the diffusion path and the corresponding energy barrier to move one hydrogen atom, initially bonded to the Pd_6 cluster, to the closest carbon chain. The energy curve of this spillover process can be seen in Figure 10. The final state with the H atom attached to a C atom is substantially more stable than the initial state. However, the activation energy is large, 1.37 eV. The first few steps correspond to the diffusion of the H atom over the surface of the palladium cluster, and the barrier maximum corresponds to a configuration where the diffusing H atom is in a bridge

https://doi.org/10.1021/acs.chemmater.2c03106
Chem. Mater. 2023, 35, 1134−1147

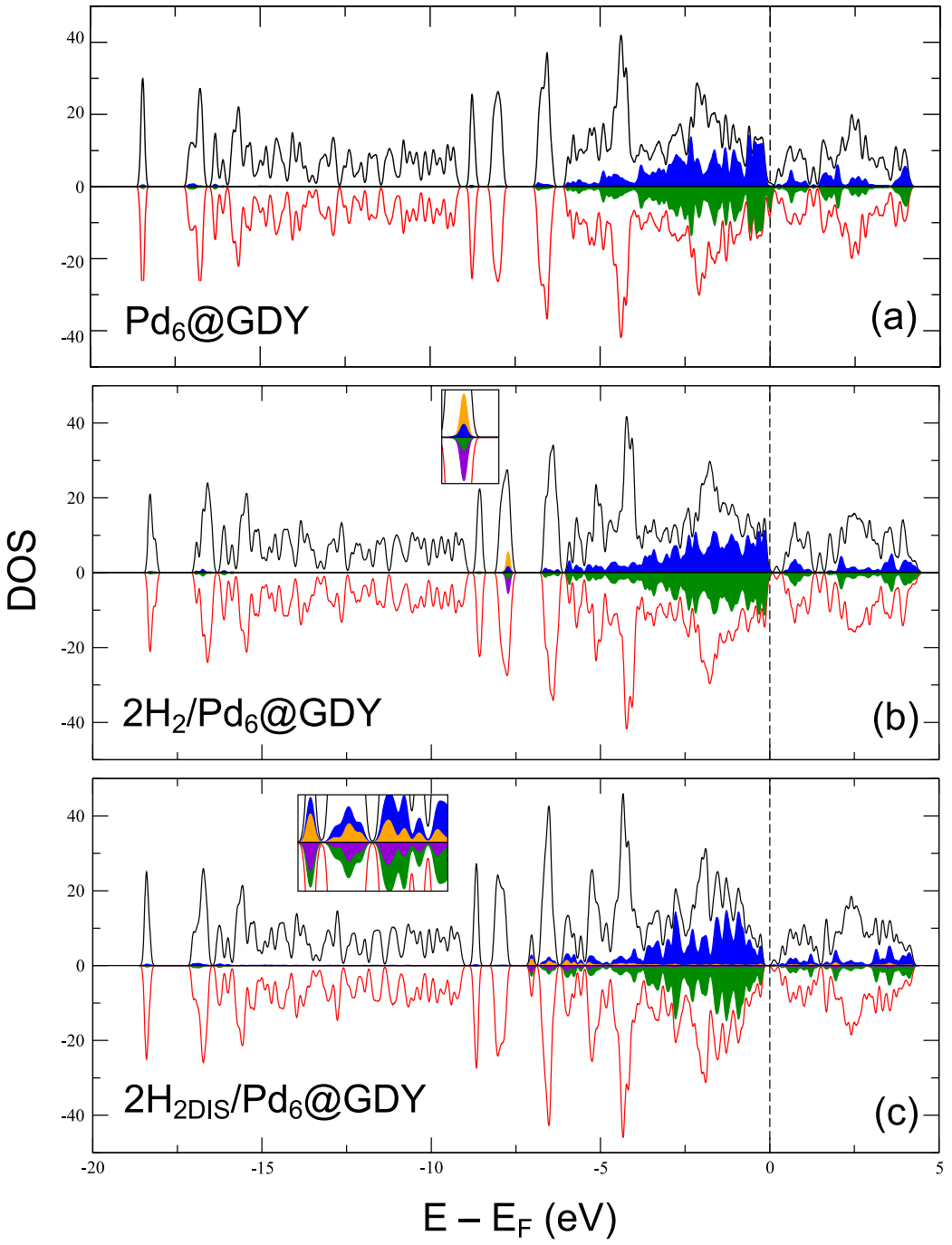

Figure 9. DOS of Pd_6GDY, 2(H_2)/Pd_6GDY, and 2(2H)/Pd_6GDY, separated in spin-up (black color) and spin-down (red color) components. Blue and green regions correspond to the DOS projected on the Pd atoms. Projections on H atoms are indicated in orange and purple.

position between a carbon atom of the carbon chain and one Pd atom (C−H−Pd intermediate); then, the energy drops once the H atom is separated from the Pd cluster and bonded to a C atom, and the hydrogenated Pd_6GDY system relaxes its structure.

In addition to the five molecules whose adsorption energies are reported in Table 1, additional H_2 molecules can be adsorbed on the Pd cluster and on the carbon chains and carbon hexagons, with adsorption energies lower than 0.09 eV and H_2−Pd (or H_2−C) distances larger than 3 Å (see also Section 5). The interest in those molecules is quite limited because their desorption is easy except at low temperatures.

7. HYDROGEN ADSORPTION ON PD_6BGDY

The lowest energy state structure of bare Pd_6BGDY is given in Figure 4. The adsorption of a hydrogen molecule on Pd_6BGDY has been studied, both in molecular and dissociated forms. The left panels of Figure 11 show the most stable molecular adsorption configuration, in which the H_2 molecule binds to atom Pd6 with an adsorption energy of 0.713 eV and Pd−H bond lengths of 1.72 Å. Molecular adsorption is also possible on other Pd atoms. Adsorption energy on Pd1 is 0.688 eV, and it is smaller on Pd2, Pd3, and Pd5 (with values 0.610, 0.242, and 0.400 eV, respectively), and adsorption is not stable on Pd4. Again, this is justified by the observation that Pd6 and

https://doi.org/10.1021/acs.chemmater.2c03106
Chem. Mater. 2023, 35, 1134−1147

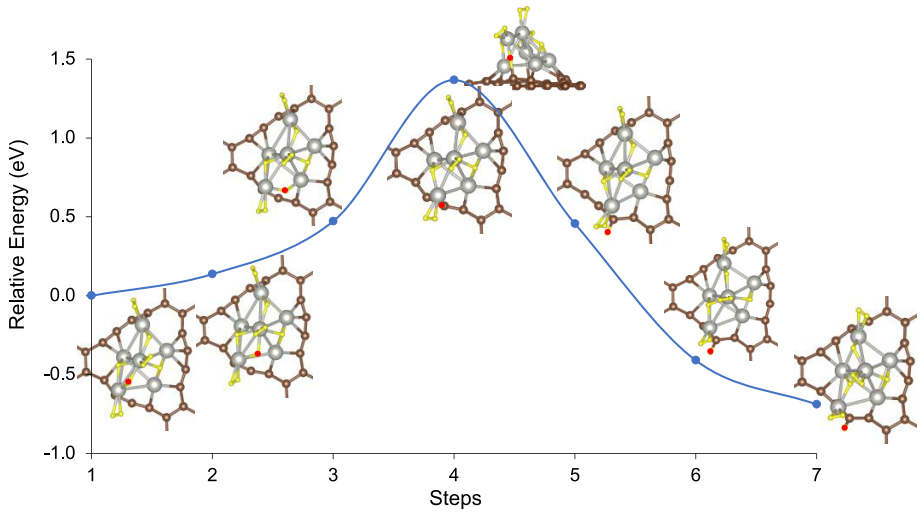

Figure 10. Energy curve and structural snapshots along the migration path of an H atom from the Pd_6 cluster saturated with hydrogen (4H + 3 H_2) toward the GDY substrate. C, Pd, and most H atoms are represented by brown, gray, and yellow spheres, respectively, but the H atom moving towards the substrate is represented in red color.

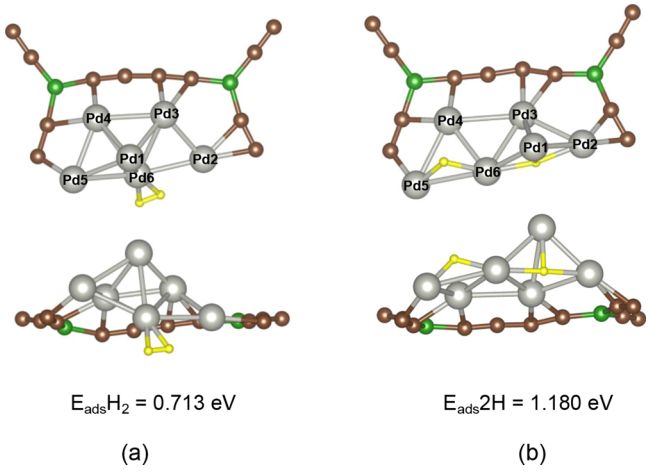

Figure 11. Molecular (a) and dissociative (b) adsorption of the first H_2 molecule on Pd_6BGDY. Top (above) and lateral (below) views are shown. C, B, Pd, and H atoms are represented by brown, green, gray, and yellow spheres, respectively.

Pd1 do not form bonds with C atoms, so atomic coordination and steric effects favor adsorption on Pd6 and Pd1. An interesting observation is that the highest adsorption energies on Pd_6BGDY (0.69−0.71 eV) are larger compared to the case of H_2 adsorption on Pd_6GDY (0.54 eV; see Figure 5). The reason is that the structure of the Pd_6 cluster is less compact in BGDY. In more quantitative terms, we can apply the concept of generalized atomic coordination numbers (CN_g) to the host Pd atoms.[70,76] To assign a CN_g to an atom i with n_i nearest neighbors, those neighbors are counted and weighted by their own usual coordination numbers CN. That is,

$$CN_g(i) = \sum_{j=1}^{n_i} \frac{\boldsymbol{CN(j)}}{\boldsymbol{CN_{max}}} \tag{8}$$

where j runs over the n_i nearest neighbors of atom i, and CN_{max} is a normalizing factor. We restrict the counting of neighbors to the Pd cluster, and CN_{max} is identified with the maximum number of neighbors in the cluster. Then, with CN_{max} = 4 for Pd_6 on GDY, we find CN_g(Pd2) = 4, because each one of the Pd atoms in the cluster has four neighbors. On the other hand, with CN_{max} = 5 for Pd_6 on BGDY, CN_g(Pd6) = 3.4, and CN_g(Pd1) = 3.2. The lower effective atomic coordination of the host Pd atoms in BGDY increases their reactivity, and higher H_2 adsorption energies then result. The bond lengths d(H−H) of the activated H_2 molecules vary between 0.88 and 0.95 Å.

To study the dissociative adsorption of the H_2 molecule, H atoms were placed in bridge positions on top of Pd−Pd bonds and on hollow triangular sites. Figure 11b shows the most stable dissociative adsorption configuration. The structure of the Pd_6 cluster is substantially deformed in comparison with the structures of clean Pd_6BGDY and Pd_6BGDY with molecular H_2, and Pd_6 becomes flatter. Only atoms Pd3 and Pd6 are coordinated to four Pd atoms, while the other Pd atoms have coordination 3 or 2. One H atom is in a bridge position above the bond Pd5−Pd6, and the other H atom shows an interesting configuration bound to Pd1, Pd2, and Pd6, forming a (nearly flat) isosceles triangle with a long Pd2−H−Pd6 base. The adsorption energy is E_{ads} (2H) = 1.180 eV. The Pd−H bond lengths are 1.73 and 1.75 Å for Pd6−H and Pd5−H, respectively, while for the case of an isosceles triangle, the bond lengths are 1.78, 1.92, and 1.90 Å for Pd1−H, Pd2−H, and Pd6−H, respectively. The activation energy barrier for hydrogen dissociation, i.e., from the structure shown in Figure 11a,b, is small, only 0.232 eV, and a few structural snapshots and their energies along a minimum energy NEB path are shown in Figure S5 of the Supporting Information. This barrier is quite small compared to the dissociation barrier of H_2 on clean BGDY (1.96 eV; see Section 5).

When a second molecule is adsorbed, the Pd cluster becomes even flatter (Figure 12a). The two adsorbed molecules are dissociated, with two H atoms on hollow triangular sites and the other two H atoms on bridge sites above Pd−Pd bonds. The adsorption energy of the second molecule is 1.165 eV, close to the value of the first molecule. A third hydrogen molecule is also dissociatively adsorbed (Figure 12b). The structure of Pd_6 does not suffer notable changes, although the tendency to form a flat ribbon continues. Two H atoms sit on hollow triangular sites and the other four on bridge sites. The adsorption energy of the third molecule is 1.175 eV. The ribbon-like form adopted by the Pd cluster fits

https://doi.org/10.1021/acs.chemmater.2c03106
Chem. Mater. 2023, 35, 1134−1147

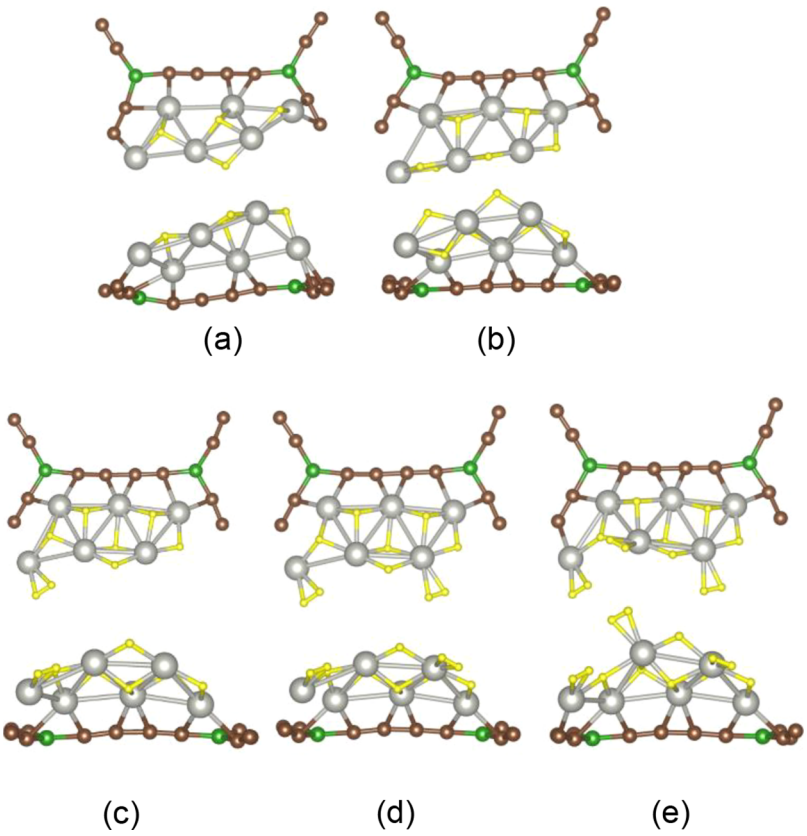

Figure 12. Minimum energy configurations of Pd_6BGDY with two (a), three (b), four (c), five (d), and six (e) adsorbed H_2 molecules. The first three molecules dissociate, and additional molecules stay in the molecular form. Top and lateral views are shown in each case. C, B, Pd, and H atoms are represented by brown, green, gray, and yellow spheres, respectively.

well into the BGDY holes, and half of the Pd atoms of the ribbon form bonds with C atoms. Bonding and steric constraints limit to three the number of dissociated H_2 molecules that the system can adsorb, and additional H_2 molecules are adsorbed in the molecular form. The structures with four, five, and six adsorbed molecules are shown in panels (c), (d), and (e) of Figure 12, respectively, and it can be noticed that the spreading of the Pd atoms over the empty area of the hole continues. The fourth, fifth, and sixth H_2 molecules are adsorbed on top of Pd atoms, and these molecules mainly point toward the central region of the hexagonal hole. A clear steric effect can be appreciated, with hydrogen atoms and molecules avoiding staying too close to each other. The adsorption energies of each newly added H_2 molecule are collected in Table 2, with a clear distinction between dissociated and nondissociated molecules. Adsorption energies larger than 0.4 eV occur for the first three nondissociated molecules. Additional molecules can be adsorbed, either on the Pd cluster (on both sides of the Pd ribbon) or on the carbon chains, with adsorption energies lower than 0.101 eV, and these low adsorption energies will be relevant for adsorption at low temperature only. Those molecules are placed at distances of 3.4 Å from C atoms, and 3.5 Å from Pd atoms. Similar results have been obtained for the adsorption of hydrogen on Pd_6 anchored to graphene vacancies:[29] three dissociated molecules and six nondissociated with adsorption energies larger than 0.1 eV.

Table 2. Adsorption of H_2 on Pd_6BGDY: Number N of Adsorbed Molecules, Adsorption Mode of the Last Molecule (Molecular or Dissociative Adsorption), and Adsorption Energy of the Last Molecule, E_{ads} (Last)

N	adsorption mode (last)	E_{ads} (last) (eV)
1	dissociated	1.181
2	dissociated	1.165
3	dissociated	1.175
4	molecular	0.648
5	molecular	0.484
6	molecular	0.441

As in the case of graphdiyne, the effect of the adsorption of hydrogen on the electronic structure of Pd_6BGDY depends on H_2 being dissociated or nondissociated. Figure S6 of the Supporting Information shows the DOS of H_2/Pd_6GDY and $(2H)/Pd_6$GDY. The electronic states of the nondissociated hydrogen molecule are well localized at an energy of 7.7 eV below the Fermi level, and in the case of the dissociated molecule, the hydrogen states are strongly hybridized with the d states of the Pd cluster.

To study the possible spillover mechanism in Pd_6BGDY saturated with hydrogen, we have calculated the diffusion path and the energy barrier to move one hydrogen atom bonded to the Pd_6 cluster to the carbon chain of the support BGDY layer. The energy curve of this process, given in Figure 13, shows that the spillover is energetically possible. That is, the final state with the H atom attached to a C atom is more stable than the initial state. However, a large activation energy of 1.34 eV is found, similar to the case of spillover on the GDY substrate (see Section 6). The first three steps in Figure 13 reveal a moderate rearrangement of the structure without breaking of

https://doi.org/10.1021/acs.chemmater.2c03106
Chem. Mater. 2023, 35, 1134−1147

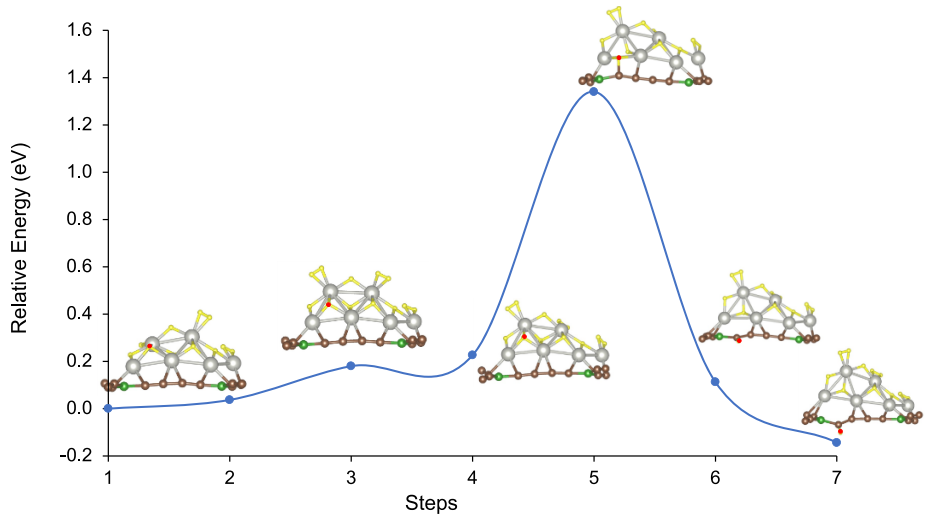

Figure 13. Energy curve and several structural snapshots along the migration path of an H atom from the Pd_6 cluster saturated with hydrogen ($6H + 3H_2$) toward the BGDY substrate. C, B, Pd, and most H atoms are represented by brown, green, gray, and yellow spheres, respectively, but the H atom moving toward the substrate is represented in red color.

bonds. The step which requires most energy consists in the breaking of one H−Pd bond of the spilling H atom (initially bonded to three Pd atoms) to form an H−C bond, while the other two H−Pd bonds remain intact. This rearrangement is accompanied by the breaking of one H−Pd bond of a neighbor H atom originally also bonded to three Pd atoms.

8. DISCUSSION

The results for hydrogen adsorption on Pd_6GDY and Pd_6BGDY indicate that the first material adsorbs five hydrogen molecules per Pd_6 cluster with adsorption energies larger than 0.01 eV, and the second material six. The first two molecules in Pd_6GDY and the first three molecules in Pd_6BGDY are adsorbed in the dissociated mode, and the rest are non-dissociated. The adsorption energies are larger on Pd_6BGDY, except for the first molecule. In both systems, the Pd atoms form bonds with the carbon atoms. Pd_6 fits tightly into the empty holes of GDY, but the holes in BGDY are larger and the Pd_6 clusters are less constrained and are able to rearrange their structure to store more hydrogen. This feature suggests building a platform formed by Pd_6 clusters anchored to the holes in BGDY, as shown in the model of Figure 14. The platform would be a two-dimensional arrangement of Pd nanohydrides where BGDY acts as a light framework to stabilize the arrangement. With one Pd_6 cluster per hexagon and six H_2 molecules adsorbed per cluster, the predicted storage is 1.5% of hydrogen in weight. This value is below the target; however, the positive message of this work is the novel approach of building a storage platform of nanohydrides. The specific value of 1.5% is a consequence of the high atomic mass of the Pd atom, 106.42 amu. Then, by building nanohydride platforms with lighter metals having a good hydrogen adsorption capacity, the storage can be enhanced substantially. A promising candidate may be cobalt. The affinity of free cobalt clusters, and cobalt clusters supported on carbon substrates, for hydrogen[77,78] is even higher than that of palladium clusters, and at the same time, the atomic mass, 58.93 amu, is much lower.

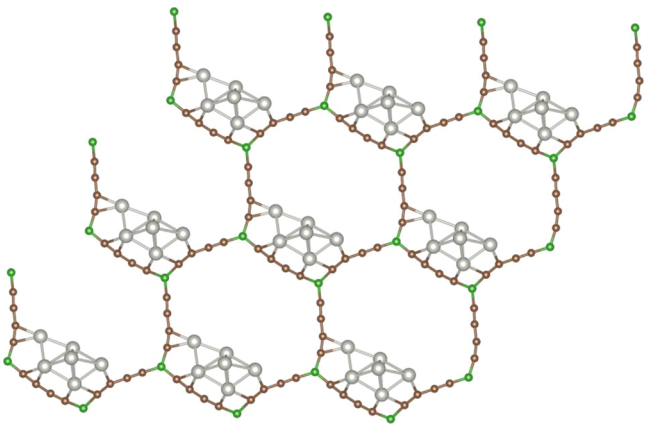

Figure 14. Model of adsorbing the platform formed by Pd clusters supported on BGDY; one cluster per hexagonal hole.

9. CONCLUSIONS

Density functional calculations have been performed to investigate the interaction of hydrogen with graphdiyne (GDY), and boron graphdiyne (BGDY), both clean and doped with Pd atoms and Pd_6 clusters. Pd_6GDY can adsorb up to five hydrogen molecules with adsorption energies larger than 0.1 eV, the first two dissociated and the rest non-dissociated. The dissociation barrier of H_2 on the deposited Pd_6 cluster is 0.58 eV, much smaller than the dissociation energy of a free H_2 molecule (4.5 eV) and also smaller than the dissociation barrier of H_2 adsorbed on clean GDY (1.62 eV). Pd_6BGDY can adsorb up to six hydrogen molecules with adsorption energies larger than 0.1 eV, the first three dissociated and the rest nondissociated. The dissociation barrier of H_2 on the deposited Pd_6 cluster is only 0.23 eV, substantially lower than the dissociation barrier on clean BGDY (1.96 eV). The adsorption energies of hydrogen are larger on Pd_6BGDY as compared to Pd_6GDY, except for the first molecule, and the reason is that the Pd_6 cluster is less constrained in the hexagonal BGDY holes. Although less relevant, additional molecules can also be adsorbed on GDY and BGDY with adsorption energies lower than 0.1 eV. We can view the Pd clusters saturated with hydrogen as nanohydrides.

https://doi.org/10.1021/acs.chemmater.2c03106
Chem. Mater. 2023, 35, 1134−1147

Spillover of the adsorbed hydrogen atoms toward the GDY and BGDY substrates is very unlikely because the activation barriers are large, 1.37 eV on Pd_6GDY and 1.34 eV on Pd_6BGDY. These results suggest using BGDY and GDY layers as support platforms for metal nanohydrides. With one Pd_6 cluster per hexagon, and assuming that each metal cluster adsorbs six hydrogen molecules, the predicted storage amounts to 1.5% of hydrogen in weight. While this value is below the target of 6%, replacing Pd by lighter metals with similar or even higher affinity for hydrogen, like cobalt, would substantially enhance the storage.

■ ASSOCIATED CONTENT

Supporting Information

The Supporting Information is available free of charge at https://pubs.acs.org/doi/10.1021/acs.chemmater.2c03106.

Minimum energy path for the structural transformation of Pd_6 adsorbed on GDY, for the dissociation path of H_2 on BGDY, and for the dissociation path of H_2 on GDY; electron density redistribution for H_2 adsorption on Pd_6GDY; and energy curve along the dissociation path of H_2 on Pd_6BGDY (PDF)

■ AUTHOR INFORMATION

Corresponding Author

Estefania German − *Departamento de Física Teórica, Atómica, y Óptica, University of Valladolid, 47011 Valladolid, Spain;* orcid.org/0000-0002-0312-8929; Email: estefania.german@uva.es

Authors

Johanna Sandoval − *Departamento de Física Teórica, Atómica, y Óptica, University of Valladolid, 47011 Valladolid, Spain*

Adrián Recio − *Departamento de Física Teórica, Atómica, y Óptica, University of Valladolid, 47011 Valladolid, Spain*

Abdolvahab Seif − *Dipartimento di Fisica e Astronomia, Universitá degli Studi Padova, Padova 35122, Italy*

Julio A. Alonso − *Departamento de Física Teórica, Atómica, y Óptica, University of Valladolid, 47011 Valladolid, Spain;* orcid.org/0000-0002-8604-8608

María J. López − *Departamento de Física Teórica, Atómica, y Óptica, University of Valladolid, 47011 Valladolid, Spain;* orcid.org/0000-0001-7698-9327

Complete contact information is available at: https://pubs.acs.org/10.1021/acs.chemmater.2c03106

Notes

The authors declare no competing financial interest.

■ ACKNOWLEDGMENTS

Work supported by Ministerio de Ciencia e Innovación of Spain (Grant PID2019-104924RB-I00 funded by MCIN/AEI/10.13039/501100011033) and the University of Valladolid (GIR Nanostructure Physics). E.G. acknowledges a postdoctoral contract with the University of Valladolid.

■ REFERENCES

(1) Marban, G.; Valdes-Solis, T. Towards the hydrogen economy? *Int. J. Hydrogen Energy* **2007**, *32*, 1625−1637.

(2) Butler, M. S.; Moran, C. W.; Sunderland, P. B.; Axelbaum, R. L. Limits for hydrogen leaks that can support stable flames. *Int. J. Hydrogen Energy* **2009**, *34*, 5174−5182.

(3) Jena, P. Materials for hydrogen storage: past, present, and future. *J. Phys. Chem. Lett.* **2011**, *2*, 206−211.

(4) Yang, R. T. Hydrogen storage by alkali-doped carbon nanotubes−revisited. *Carbon* **2000**, *38*, 623−626.

(5) Kim, B.-J.; Lee, Y.-S.; Park, S.-J. Preparation of platinum-decorated porous graphite nanofibers, and their hydrogen storage behaviors. *J. Colloid Interface Sci.* **2008**, *318*, 530−533.

(6) Bhat, V. V.; Contescu, C. I.; Gallego, N. C.; Baker, F. S. Atypical hydrogen uptake on chemically-activated, ultramicroporous carbon. *Carbon* **2010**, *48*, 1331−1340.

(7) Contescu, C. I.; van Benthem, K.; Li, S.; Bonifacio, C. S.; Pennycook, S. J.; Jena, P.; Gallego, N. C. Single Pd atoms in activated carbon fibers and their contribution to hydrogen storage. *Carbon* **2011**, *49*, 4050−4058.

(8) Tozzini, V.; Pellegrini, V. Prospects for hydrogen storage in graphene. *Phys. Chem. Chem. Phys.* **2013**, *15*, 80−89.

(9) Zhou, C.; Szpunar, J. A.; Cui, X. Synthesis of Ni/graphene nanocomposite for hydrogen storage. *ACS Appl. Mater. Interfaces* **2016**, *8*, 15232−15241.

(10) Liu, E.; Gao, Y.; Zhao, N.; Li, J.; He, C.; Shi, C. Adsorption of hydrogen atoms on graphene with TiO_2 decoration. *J. Appl. Phys.* **2013**, *113*, No. 153708.

(11) Lu, J.; Guo, Y.; Zhang, Y.; Cao, J. Li decorated 6,6,12-graphyne: A new star for hydrogen storage material. *Int. J. Hydrogen Energy* **2014**, *39*, 17112−17117.

(12) Alonso, J. A.; López, M. J. Palladium clusters, free and supported on surfaces, and their applications in hydrogen storage. *Phys. Chem. Chem. Phys.* **2022**, *24*, 2729−2751.

(13) Pyle, D. S.; Gray, E. M.; Webb, C. J. Hydrogen storage in carbon nanostructures via spillover. *Int. J. Hydrogen Energy* **2016**, *41*, 19098−19113.

(14) Blanco-Rey, M.; Juaristi, J. I.; Alducin, M.; López, M. J.; Alonso, J. A. Is spillover relevant for hydrogen adsorption and storage in porous carbons doped with palladium nanoparticles? *J. Phys. Chem. C* **2016**, *120*, 17357−17364.

(15) Granja-DelRio, A.; Alducin, M.; Juaristi, J. I.; Lopez, M. J.; Alonso, J. A. Absence of spillover of hydrogen adsorbed on small palladium clusters anchored to graphene vacancies. *Appl. Surf. Sci.* **2021**, *559*, No. 149835.

(16) Psofogiannakis, G. M.; Froudakis, G. E. DFT study of the hydrogen spillover mechanism on Pt-doped graphite. *J. Phys. Chem. C* **2009**, *113*, 14908−14915.

(17) Wu, H. Y.; Fan, X.; Kuo, J. L.; Deng, W. Q. DFT study of hydrogen storage by spillover on graphene with boron substitution. *J. Phys. Chem. C* **2011**, *115*, 9241−9249.

(18) Juarez-Mosqueda, R.; Mavrandonakis, A.; Kuc, A. B.; Pettersson, L. G. M.; Heine, T. Theoretical analysis of hydrogen spillover mechanism on carbon nanotubes. *Front. Chem.* **2015**, *3*, 2.

(19) Ambrusi, R. E.; Orazi, V.; Marchetti, J. M.; Juan, A.; Pronsato, M. E. Hydrogen storage by spillover on Ni_4 cluster embedded in three vacancy graphene. A DFT and dynamics study. *J. Phys. Chem. Solids* **2022**, *167*, No. 110706.

(20) Fang, J.; Levchenko, I.; Lu, X.; Mariotti, D.; Ostrikov, K. Hierarchical bi-dimensional alumina/palladium nanowire nano-architectures for hydrogen detection, storage and controlled release. *Int. J. Hydrogen Energy* **2015**, *40*, 6165−6172.

(21) Züttel, A.; Wenger, P.; Sudan, P.; Mauron, P.; Orimo, S. Hydrogen density in nanostructured carbon, metals and complex materials. *Mater. Sci. Eng., B* **2004**, *108*, 9−18.

(22) Watari, N.; Ohnishi, S.; Ishii, Y. Hydrogen storage in Pd clusters. *J. Phys.: Condens. Matter* **2000**, *12*, 6799−6823.

(23) Huang, H.; Bao, S.; Chen, Q.; Yang, Y.; Jiang, Z.; Kuang, Q.; Wu, X.; Xie, Z.; Zheng, L. Novel hydrogen storage properties of palladium nanocrystals activated by a pentagonal cyclic twinned structure. *Nano Res.* **2015**, *8*, 2698−2705.

(24) Valencia, F. J.; González, R. I.; Tramontina, D.; Rogan, J.; Valdivia, J. A.; Kiwi, M.; Bringa, E. M. Hydrogen storage in palladium hollow nanoparticles. *J. Phys. Chem. C* **2016**, *120*, 23836−23841.
(25) Chen, B. W. J.; Mavrikakis, M. Effects of composition and morphology on the hydrogen storage properties of transition metal hydrides: Insights from PtPd nanoclusters. *Nano Energy* **2019**, *63*, No. 103858.
(26) Cabria, I.; López, M. J.; Fraile, S.; Alonso, J. A. Adsorption and dissociation of molecular hydrogen on palladium clusters supported on graphene. *J. Phys. Chem. C* **2012**, *116*, 21179−21189.
(27) Lopez-Corral, I.; German, E.; Juan, A.; Volpe, M. A.; Brizuela, G. P. DFT study of hydrogen adsorption on palladium decorated graphene. *J. Phys. Chem. C* **2011**, *115*, 4315−4323.
(28) López-Corral, I.; de Celis, J.; Juan, A.; Irigoyen, B. DFT study of H_2 adsorption on Pd-decorated single walled carbon nanotubes with C-vacancies. *Int. J. Hydrogen Energy* **2012**, *37*, 10156−10164.
(29) Granja, A.; Alonso, J. A.; Cabria, I.; López, M. J. Competition between molecular and dissociative adsorption of hydrogen on palladium clusters deposited on defective graphene. *RSC Adv.* **2015**, *5*, 47945−47953.
(30) Wenelska, K.; Michalkiewicz, B.; Chen, X.; Mijowska, E. Pd nanoparticles with tunable diameter deposited on carbon nanotubes with enhanced hydrogen storage capacity. *Energy* **2014**, *75*, 549−554.
(31) Ramos-Castillo, C. M.; Reveles, J. U.; Zope, R. R.; de Coss, R. Palladium clusters supported on graphene monovacancies for hydrogen storage. *J. Phys. Chem. C* **2015**, *119*, 8402−8409.
(32) Franz, D.; Schröder, U.; Shayduk, R.; Arndt, B.; Noei, H.; Vonk, V.; Michely, T.; Stierle, A. Hydrogen solubility and atomic structure of graphene supported Pd nanoclusters. *ACS Nano* **2021**, *15*, 15771−15780.
(33) Ferrante, F.; Prestianni, A.; Bertini, M.; Duca, D. H_2 transformations on graphene supported palladium cluster: DFT-MD simulations and NEB calculations. *Catalysts* **2020**, *10*, 1306.
(34) Rangel, E.; Sansores, E.; Vallejo, E.; Hernández-Hernández, A.; López-Pérez, P. A. Study of the interplay between N-graphene defects and small Pd clusters for enhanced hydrogen storage via a spill-over mechanism. *Phys. Chem. Chem. Phys.* **2016**, *18*, 33158.
(35) Gao, X.; Liu, H.; Wang, D.; Zhang, J. Graphdiyne: synthesis, properties, and applications. *Chem. Soc. Rev.* **2019**, *48*, 908−936.
(36) Du, Y.; Zhou, W.; Gao, J.; Pan, X.; Li, Y. Fundament and application of graphdiyne in electrochemical energy. *Acc. Chem. Res.* **2020**, *53*, 459−469.
(37) Seif, A.; López, M. J.; Granja-Del Río, A.; Azizi, K.; Alonso, J. A. Adsorption and growth of palladium clusters on graphdiyne. *Phys. Chem. Chem. Phys.* **2017**, *19*, 19094.
(38) Wang, N.; Li, X.; Tu, Z.; Zhao, F.; He, J.; Guan, Z.; Huang, C.; Yi, Y.; Li, Y. Synthesis, electronic structure of boron−graphdiyne with an sp-hybridized carbon skeleton and its application in sodium storage. *Angew. Chem., Int. Ed.* **2018**, *57*, 3968−3973.
(39) German, E.; Alvarez-Yenes, A.; Alonso, J. A.; López, M. J. Adsorption of transition metal clusters on boron-graphdiyne. *Appl. Surf. Sci.* **2021**, *548*, No. 149270.
(40) Panigrahi, P.; Dhinakaran, A. K.; Naqvi, S. R.; Gollu, S. R.; Ahuja, R.; Hussain, T. Light metal decorated graphdiyne nanosheets for reversible hydrogen storage. *Nanotechnology* **2018**, *29*, 35540.
(41) Hussain, T.; Mortazavi, B.; Bae, H.; Rabczuk, T.; Lee, H.; Karton, A. Enhancement in hydrogen storage capacities of light metal functionalized boron-graphdiyne nanosheets. *Carbon* **2019**, *147*, 199−205.
(42) Dehkhodaei, M.; Reisi-Vanani, A. Effect of the charge injection and N and S co-doping on the structural and electronic properties, and hydrogen storage capacity of graphdiyne 2D structure. *Surf. Interfaces* **2022**, *31*, No. 102031.
(43) Akbari, F.; Reisi-Vanani, A.; Darvishnejad, M. H. DFT study of the electronic and structural properties of single Al and N atoms and Al-N co-doped graphyne toward hydrogen storage. *Appl. Surf. Sci.* **2019**, *488*, 600−610.
(44) Kwon, Y.; Kim, J.; Kim, T.; Shin, H. S.; Kwon, S. Effect of bimodal surface modification of graphyne on enhanced H_2 storage: Density functional theory study. *AIP Adv.* **2018**, *8*, No. 115034.
(45) Zhang, Y.; Zhang, L.; Pan, H.; Wang, H.; Li, Q. Li-decorated porous hydrogen substituted graphyne: A new member of promising hydrogen storage medium. *Appl. Surf. Sci.* **2021**, *535*, No. 147683.
(46) Hussain, T.; Hankel, M.; Searles, D. J. Graphenylene monolayers doped with alkali or alkaline earth metals: Promising materials for clean energy storage. *J. Phys. Chem. C* **2017**, *121*, 14393−14400.
(47) Wang, Y.; Wu, Q.; Mao, J.; Deng, S.; Ma, R.; Shi, J.; Ge, J.; Huang, X.; Bi, L.; Yin, J.; Ren, S.; Yan, G.; Yang, Z. Lithium and calcium decorated triphenylene-graphdiyne as potential high-capacity hydrogen storage medium: A first-principles prediction. *Appl. Surf. Sci.* **2019**, *494*, 763−770.
(48) Shen, S.; Hu, Z.; Zhang, H.; Song, K.; Wang, Z.; Lin, Z.; Zhang, Q.; Gu, L.; Zhong, W. Highly active Si sites enabled by negative valent Ru for electrocatalytic hydrogen evolution in LaRuSi. *Angew. Chem., Int. Ed.* **2022**, *61*, No. e202206460.
(49) Ma, S.; Deng, J.; Xu, Y.; Tao, W.; Wang, X.; Lin, Z.; Zhang, Q.; Gu, L.; Zhong, W. Pollen-like self-supported FeIr alloy for improved hydrogen evolution reaction in acid electrolyte. *J. Energy Chem.* **2022**, *66*, 560−565.
(50) Contescu, C. I.; Brown, C. M.; Liu, Y.; Bhat, V. V.; Gallego, N. C. Detection of hydrogen spillover in palladium-modified activated carbon fibers during hydrogen adsorption. *J. Phys. Chem. C* **2009**, *113*, 5886−5890.
(51) van Benthem, K.; Bonifacio, C. S.; Contescu, C. I.; Gallego, N. C.; Pennycook, S. J. STEM imaging of single Pd atoms in activated carbon fibers considered for hydrogen storage. *Carbon* **2011**, *49*, 4059−4063.
(52) Bhat, V. V.; Contescu, C. I.; Gallego, N. C. Kinetic effect of Pd additions on the hydrogen uptake of chemically-activated ultra-microporous carbon. *Carbon* **2010**, *48*, 2361−2364.
(53) Bhat, V. V.; Contescu, C. I.; Gallego, N. C. The role of destabilization of palladium hydride in the hydrogen uptake of Pd-containing activated carbons. *Nanotechnology* **2009**, *20*, No. 204011.
(54) Kohn, W.; Sham, L. J. Self-consistent equations including exchange and correlation effects. *Phys. Rev.* **1965**, *140*, A1133−A1138.
(55) Jain, A.; Shin, Y.; Persson, K. A. Computational predictions of energy materials using density functional theory. *Nat. Rev. Mater.* **2016**, *1*, 15004.
(56) Penev, E. S.; Marzari, N.; Yakobson, B. I. Theoretical prediction of two-dimensional materials, behavior, and properties. *ACS Nano* **2021**, *15*, 5959−5976.
(57) Giannozzi, P.; Baroni, S.; Bonini, N.; Calandra, M.; Car, R.; Cavazzoni, C.; Ceresoli, D.; Chiarotti, G. L.; Cococcioni, M.; Dabo, I.; et al. QUANTUM ESPRESSO: a modular and open-source software project for quantum simulations of materials. *J. Phys.: Condens. Matter* **2009**, *21*, No. 395502.
(58) https://www.quantumespresso.org.
(59) Perdew, J. P.; Burke, K.; Ernzerhof, M. Generalized gradient approximation made simple. *Phys. Rev. Lett.* **1996**, *77*, 3865−3868.
(60) Kresse, G.; Joubert, D. From ultrasoft pseudopotentials to the projector augmented wave method. *Phys. Rev. B* **1999**, *59*, 1758−1775.
(61) Blöchl, P. E. Projector augmented-wave method. *Phys. Rev. B* **1994**, *50*, 17953−17979.
(62) Grimme, S.; Antony, J.; Ehrlich, S.; Krieg, H. A consistent and accurate ab initio parametrization of density functional dispersion correction (DFT-D) for the 94 elements H-Pu. *J. Chem. Phys.* **2010**, *132*, No. 154104.
(63) Goerigk, L. A comprehensive overview of the DFT-D3 London-dispersion correction. In *Non-Covalent Interactions in Quantum Chemistry and Physics*, Otero de la Roza, A.; DiLabio, G. A., Eds; Elsevier, 2017; pp 195−219
(64) Monkhorst, H. J.; Pack, J. D. Special points for Brillouin-zone integrations. *Phys. Rev. B* **1976**, *13*, 5188−5192.

(65) Narita, N.; Nagai, S.; Suzuki, S.; Nakao, K. Optimized geometries and electronic structures of graphyne and its family. *Phys. Rev. B* **1998**, *58*, 11009−11014.
(66) Bromann, K.; Félix, C.; Brune, H.; Harbich, W.; Monot, R.; Buttetand, J.; Kern, K. Controlled deposition of size-selected silver nanoclusters. *Science* **1996**, *274*, 956−958.
(67) Henkelman, G.; Uberuaga, B. P.; Jónsson, H. A climbing image nudged elastic band method for finding saddle points and minimum energy paths. *J. Chem. Phys.* **2000**, *113*, 9901−9904.
(68) Granja-Del Río, A.; Alonso, J. A.; López, M. J. Steric and chemical effects on the hydrogen adsorption and dissociation on free and graphene-supported palladium clusters. *Comput. Theoret. Chem.* **2017**, *1107*, 23−29.
(69) Alducin, M.; Juaristi, J. I.; Granja-Del Río, A.; López, M. J.; Alonso, J. A. Dynamics of cluster isomerization induced by hydrogen adsorption. *J. Phys. Chem. C* **2019**, *123*, 15236−15243.
(70) Ortega, G.; Germán, E.; López, M. J.; Alonso, J. A. Catalytic activity of Co-Ag nanoalloys to dissociate molecular hydrogen. New insights on the chemical environment. *Int. J. Hydrogen Energy* **2022**, *47*, 19038−19050.
(71) Cabria, I.; López, M. J.; Alonso, J. A. Enhancement of hydrogen physisorption on graphene and carbon nanotubes by Li doping. *J. Chem. Phys.* **2005**, *123*, No. 204721.
(72) Cabria, I.; López, M. J.; Alonso, J. A. Searching for DFT-based methods that include dispersion interactions to calculate the physisorption of H_2 on benzene and graphene. *J. Chem. Phys.* **2017**, *146*, No. 214104.
(73) Bores, C.; Cabria, I.; Alonso, J. A.; López, M. J. Adsorption and dissociation of molecular hydrogen on the edges of graphene nanoribbons. *J. Nanopart. Res.* **2012**, *14*, 1263.
(74) Granja-Del Río, A.; Alonso, J. A.; López, M. J. Competition between palladium clusters and hydrogen to saturate graphene vacancies. *J. Phys. Chem. C* **2017**, *121*, 10843−10850.
(75) Kleis, J.; Greeley, J.; Romero, N. A.; Morozov, V. A.; Falsig, H.; Larsen, A. H.; Lu, J.; Mortensen, J. J.; Dulak, M.; Thygesen, K. S.; Norskov, J. K.; Jacobsen, K. W. Finite size effects in chemical bonding: from small clusters to solids. *Catal. Lett.* **2011**, *141*, 1067−1071.
(76) Calle-Vallejo, F.; Martínez, J. I.; García-Lastra, J. M.; Sautet, P.; Loffreda, D. Fast prediction of adsorption properties for platinum nanocatalysts with generalized coordination numbers. *Angew. Chem., Int. Ed.* **2014**, *53*, 8316−8319.
(77) García-Díez, K.; Fernández-Fernández, J.; Alonso, J. A.; López, M. J. Theoretical study of the adsorption of hydrogen on cobalt clusters. *Phys. Chem. Chem. Phys.* **2018**, *20*, 21163−21176.
(78) Germán, E.; Alonso, J. A.; Janssens, E.; López, M. J. $C_{60}Co_n$ complexes as hydrogen adsorbing materials. *Int. J. Hydrogen Energy* **2021**, *46*, 20594−20606.

https://doi.org/10.1021/acs.chemmater.2c03106
Chem. Mater. 2023, 35, 1134−1147